Long-distance axonal regeneration induced by CNTF gene transfer is impaired by axonal misguidance in the injured adult optic nerve

Vincent Pernet [a,*], Sandrine Joly [a], Deniz Dalkara [b], Noémie Jordi [a], Olivia Schwarz [a], Franziska Christ [a], David V. Schaffer [b], John G. Flannery [c], Martin E. Schwab [a]

[a] Brain Research Institute, University of Zürich, and Dept of Health Sciences and Technology, ETH Zürich, Winterthurerstrasse 190, CH-8057 Zürich, Switzerland
[b] Dept of Chemical Engineering, Dept of Bioengineering, and Helen Wills Neuroscience Institute, University of California at Berkeley, Berkeley, CA 94720, USA
[c] Dept of Molecular and Cellular Biology and Helen Wills Neuroscience Institute, University of California at Berkeley, Berkeley, CA 94720, USA

ARTICLE INFO

ABSTRACT

The optic nerve crush injury is a well-accepted model to study the mechanisms of axonal regeneration after trauma in the CNS. The infection of retinal ganglion cells (RGCs) with an adeno-associated virus serotype 2 — ciliary neurotrophic factor (AAV2.CNTF) was previously shown to stimulate axonal regeneration. However, the transfection of axotomized neurons themselves may not be optimal to promote full axonal regeneration in the visual system. Here, we show that the release of CNTF by glial cells is a very powerful stimulus for optic fiber regeneration and RGC survival after optic nerve crush. After 8 weeks, long-distance regeneration of severed optic axons was induced by CNTF until and beyond the optic chiasm. Regenerated axons stayed for at least 6 months in the damaged optic nerve. Strikingly, however, many regenerated axons showed one or several sharp U-turns along their course, suggesting that guidance cues are missing and that long-distance axonal regeneration is limited by the return of the growing axons toward the retina. Even more surprisingly, massive axonal sprouting was observed within the eye, forming a dense plexus of neurites at the inner surface of the retina. These results indicate that massive stimulation of the neuronal growth program can lead to aberrant growth; the absence of local regulatory and guidance factors in the adult, injured optic nerve may therefore represent a major, so far underestimated obstacle to successful axon regeneration.

© 2012 Elsevier Inc. All rights reserved.

Introduction

The optic nerve crush model was extensively used to study the mechanisms of axonal growth inhibition and to design new repair strategies for the injured CNS (Benowitz and Yin, 2007; Harvey et al., 2006). In the intraorbital optic nerve crush paradigm, severed axons cannot spontaneously regenerate into the distal part of the optic nerve and most of the retinal ganglion cell (RGC) bodies die by apoptosis after 2 weeks (Berkelaar et al., 1994).

Contrary to BDNF (Mansour-Robaey et al., 1994) or FGF2 (Sapieha et al., 2003), CNTF was shown to stimulate both axonal regeneration and neuronal survival after optic nerve lesion (Lingor et al., 2008; Muller et al., 2007, 2009). Repeated intraocular injections of the recombinant CNTF peptide were efficient at activating axonal growth and neuronal survival but only to a limited extent (Muller et al., 2007). The effects of CNTF are likely restricted in time by the short

half life of the recombinant peptide (Dittrich et al., 1994) and by the negative feedback control mediated by the up-regulation of the *suppressor of cytokine signaling 3* (SOCS3) (Smith et al., 2009). To sustain the CNTF delivery in the retina, an adeno-associated virus serotype 2 (AAV2) containing the *Cntf* cDNA was intravitreally injected to selectively infect the RGCs. AAV2.CNTF treatment resulted in significant neuroprotection and regeneration of some optic axons over longer distances (Leaver et al., 2006a,b). However, transducing neurons may not be optimal to deliver survival factors to the retina as only a small number of cells was infected (Leaver et al., 2006b) and protein synthesis is altered in axotomized neurons (Park et al., 2008).

Here, we hypothesized that the Müller glia-mediated release of CNTF may improve neuroprotection and stimulate long-distance axonal regeneration. In the healthy retina, Müller cells fulfill similar homeostatic functions as astrocytes in the rest of the CNS (Bringmann et al., 2006). Müller cell bodies occupy a central position in the retina from where they extend radial processes contacting all types of retinal neurons. In the degenerating retina, Müller cells are resistant to cell death and therefore are ideal intermediates to release neurotrophic factors. After optic nerve lesion, the Müller cell response is characterized by strong reactive gliosis and by a small number of proliferating cells (Wohl et al., 2009). AAVs allow stable, safe and efficient gene transfer and are thus suitable for human gene therapy (Bainbridge et al., 2008;

* Corresponding author at: Brain Research Institute, University of Zürich/ETH, Winterthurerstrasse, 190, Room 55J34a, CH-8057 Zürich, Switzerland. Fax: +41 44 635 33 03.
E-mail address: pernet@hifo.uzh.ch (V. Pernet).

Available online on ScienceDirect (www.sciencedirect.com).

Maguire et al., 2008, 2009). An engineered AAV called ShH10 was selected based on its ability to preferentially transduce Müller glia (Klimczak et al., 2009). Here we present the effects of the infection of Müller cells by the ShH10 vector carrying the cDNA of DH-CNTF, a mutant peptide exhibiting a higher affinity for CNTFRα and therefore acting as a super-agonist for this receptor subunit (Saggio et al., 1995). Our results show that glia-targeting AAV.DH-CNTF can promote long-range axonal regeneration. However, the distance covered by the regrowing axons was severely limited by the frequent formation of U-turns in the optic nerve. In addition, we observed massive aberrant axonal sprouting at the inner surface of the retina. Our data suggest that axonal misguidance is a key limiting factor for the long-distance axonal regeneration in the visual system.

Materials and methods

Animals

All surgeries were performed on 2–4 month old male C57BL/6 mice. Animal experiments were performed in agreement with the guidelines of the Veterinary Office of the Canton of Zürich.

ShH10 vector production

The AAV transfer plasmid with a modified form of the ciliary neurotrophic factor gene, DH-CNTF (Fig. 1C) was a generous gift from Dr W. Hauswirth, University of Florida. DH-CNTF recognizes with higher affinity the CNTFRα (Saggio et al., 1995) subunit (Fig. 1C). This construct contained a growth hormone signal peptide to improve the secretion of the CNTFRα superagonist DH-CNTF into the retina. Adeno-associated viral vectors were produced by standard methods. Triple plasmid co-transfection method (Grieger et al., 2006) was followed by ultracentrifugation as previously described (Dalkara et al., 2009). The iodixanol fraction interphase was then extracted and diluted with PBS plus 0.001% Tween 20. This fraction was buffer-exchanged and concentrated using Amicon Ultra-15 Centrifugal Filter Units to a final volume of 100–200 μL. Vector was then titered for DNase-resistant vector genomes by Real-Time qPCR relative to standards. Vector concentrations were calculated in viral genomes/mL with ShH10.GFP and ShH10.DH-CNTF at ~10^{13} vg/mL and AAV2.GFP at 1.8×10^{13} vg/mL. Four weeks after virus delivery, the infectivity of ShH10.GFP was estimated on retinal crossections in 3 different mice (3 tissue sections/mouse). On average, $84 \pm 3\%$ (mean ± S.E.M.) of glutamine synthase-positive Müller cells expressed the GFP protein.

Intraocular injections

ShH10 vectors or the anterograde tracer cholera toxin β subunit conjugated to alexa-594 (CTb, Molecular Probes) were injected as previously described (Pernet et al., 2005). To infect the Müller cells, 1 μL of ShH10.DH-CNTF or ShH10.GFP was intravitreously injected 4 weeks before optic nerve crush or tissue analysis, a time that allowed optimal transgene expression in vivo (Cheng et al., 2002; Klimczak et al., 2009).

Neuronal survival and soma diameter measurement

RGC survival was examined after intraorbital optic nerve crush injury at ~0.5 mm from the back of the eye. Two weeks after injury the animals were intracardially perfused with 4% paraformaldehyde (PFA). The RGCs were observed by immunofluorescent staining for β3Tubulin on retinal flat-mounts. β3Tubulin has previously been shown to be a specific and reliable marker to label all RGCs (Cui et al., 2003). To do so, the primary antibody was diluted in a solution of PBS containing 0.3% of Triton-X-100, 5% of normal serum and 0.05% sodium azide to prevent bacterial contamination. Then, after washings the retinae were incubated for 3 days with a goat anti-mouse secondary antibody coupled to alexa 594 or Cy3 at 4 °C. The β3Tubulin-positive RGCs were imaged in the 4 quadrants of the retina using a Leica SPE-II confocal microscope equipped with a 40× oil immersion objective (NA 1.25). Image stacks were acquired in the ganglion cell layer with a step size of 0.5 μm and a resolution of 1,024×1,024 pixels (0.27 μm/ pixel). The number of RGC cell bodies was quantified in grids of 62,500 μm² at 1 mm and 1.5 mm from the optic disk. The density of surviving RGCs was calculated in individual quadrants or in the whole retina per mm².

Axonal regeneration analysis

To study axonal regeneration, a knot was tied with a 9-0 suture to fully constrict and crush the optic nerve intraorbitally. The suture was then carefully removed and a fundus examination allowed us to control the retinal blood supply from the ophthalmic artery. One day before fixation with paraformaldehyde (4%), the optic axons were anterogradely traced by injecting 1.5 μl of 0.5% CTb into the vitreous body. Axons labeled with CTb-594 were visualized on longitudinal sections of optic nerve (14 μm) with a Zeiss Axioskop 2 Plus microscope (Carl Zeiss) and images were taken with a CCD video camera at 20×. The number of growing axons per optic nerve was estimated at 500 μm, 750 μm, 1,000 μm, 1,250 μm, 1,500 μm, 2,000 μm, 3,000 μm and 4,000 μm after the crush site (Pernet et al., 2005). Optic nerve slices were examined in 3–6 animals per condition. An estimation of the number of axons per optic nerve (Σ) was calculated with the following formula: $\Sigma_d = \Pi \times R^2 \times$ (average number of axons/mm) /T. The sum (Σ) of axons at a given distance (d) was obtained using the average optic nerve radius (R) of all optic nerves, and a thickness (T) of the tissue slices of 14 μm (Leon et al., 2000). For statistical analysis, an ANOVA followed by a Bonferroni's or Dunnett's *post hoc* test was applied for multiple comparisons. Animals presenting ischemia or retinal hemorrhages were excluded from the analysis.

For the study of ShH10.DH-CNTF-induced axonal regeneration at 6 months post-lesion, RGCs were infected by injecting 1 μL of AAV2.GFP. GFP-filled axons were examined in whole-mounted optic nerves with a Leica SPE-II confocal microscope equipped with a 40× oil immersion objective (NA 1.25) or a 10× objective (NA 0.3). Three-dimensional (3D) image stacks were reconstructed with the Imaris software (Bitplane AG, Zürich, Switzerland).

Retina, optic nerve processing and immunofluorescence

Adult mice were sacrificed by injecting an overdose of anesthetic intraperitoneally. After intracardiac perfusion with PBS (0.1 M) and 4% PFA, the eyes were rapidly dissected by removing the cornea and the lens. For retinal crossections, the eye cups were postfixed in 4% PFA overnight at 4 °C. The tissues were then cryoprotected in 30% sucrose overnight and frozen in OCT compound (optimal cutting temperature, Tissue-TEK, Sakura) with a liquid nitrogen-cooled bath of 2-methylbutane. Optic nerves and retinal sections were cut (14 μm) with a cryostat and collected on Superfrost Plus slides (Menzel-Glaser). For immunohistochemistry procedure, tissue slices were blocked with 5% BSA or normal serum, 0.3% Triton X-100 in PBS for 1 h at room temperature to avoid unspecific cross-reactivity. Then, primary antibodies were applied in 5% BSA or normal serum, 0.3% Triton X-100 in PBS overnight at 4 °C. After PBS washes, sections were incubated with the appropriate secondary antibody for 1 h at room temperature, and mounted with MOWIOL anti-fading medium (10% Mowiol 4–88 (w/v) (Calbiochem), in 100 mM Tris, pH 8.5. 25% glycerol (w/v) and 0.1% 1,4-diazabicyclo[2.2.2]octane (DABCO)). Primary antibodies were: rabbit anti-Phospho-Stat3 (1:100, Cell Signaling, #9131), rabbit anti-glial fibrillary acidic protein (GFAP, 1:500, Dako, #20334), rabbit anti-β3Tubulin (1:1,000, abcam, #ab18207), mouse anti-glutamine synthetase (GS, 1:200-1:400, Chemicon, #MAB302), mouse anti-β3Tubulin
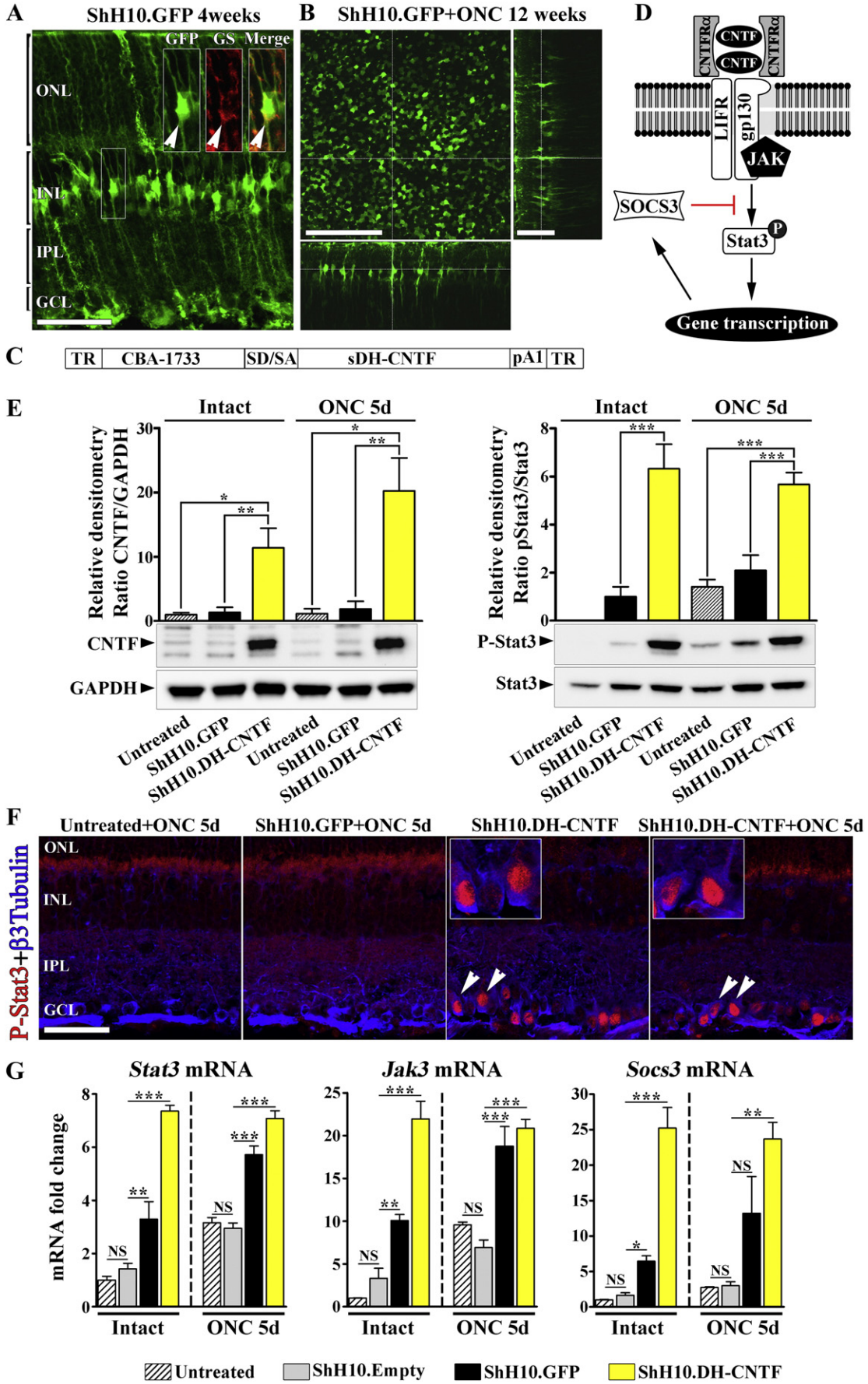
Table 1
Primer sequences used for semi-qRT-PCR.

Gene	Forward (5′-3′)	Reverse (5′-3′)	Annealing temp (°C)	Product (bp)
Gapdh	CAGCAATGCATCCTGCACC	TGGACTGTGGTCATGAGCCC	58	96
Gfap	CCACCAAACTGGCTGATGTCTAC	TTCTCTCCAAATCCACACGAGC	62	240
Jak3	GGAAGTCCTCCTGAAGGTCA	GCCGGCTTCCAGAAAAGACT	60	66
Rpl19	TGAGTATGCTCAGGCTACAG	GAATGGACAGTCACAGGCTT	62	175
Socs3	ATTTCGCTTCGGGACTAGC	AACTTGCTGTGGGTGACCAT	58	126
Stat3	CAAAACCCTCAAGAGCCAAGG	TCACTCACAATGCTTCTCCGC	62	139
Vim	TACAGGAAGCTGCTGGAAGG	TGGGTGTCAACCAGAGGAA	62	113

(1:1,000, Promega, #G712A), rabbit anti-Sox9 (1:500, Millipore, #AB5535). Immunofluorescent labelings were analyzed with a Leica SPE-II confocal microscope equipped with a 40× oil immersion objective (NA 1.25).

For the examination of intraocular axonal outgrowth at 6 months post injury, the blood vessels were labeled by intracardial perfusion with lectin-FITC (*Lycopersicon esculentum*, 1 mg/100 mL, Sigma, #L0401) in PBS as previously described (Jahrling et al., 2009).

Semi-quantitative real time RT-PCR (qRT-PCR)

After cervical dislocation, retinae were rapidly dissected in RNA Later solution (Ambion), placed in eppendorf tubes, flash frozen in liquid nitrogen and stored at −80 °C until RNA extraction. Total retinal RNA was prepared using the RNeasy RNA isolation kit (Qiagen, Hilden, Germany) including a DNase treatment to digest residual genomic DNA. For reverse transcription, equal amounts of total RNA were transformed by oligo(dT) and M-MLV reverse transcriptase (Promega, Madison, WI, USA). Ten nanograms of cDNA were amplified in the Light Cycler 480 thermocycler (Roche Diagnostics AG, Rotkreuz, Switzerland) with the polymerase ready mix (SYBR Green I Master; Roche Diagnostics AG). The appropriate primer pairs were designed to span intronic sequences or to cover exon-intron boundaries (Table 1). The analysis of the melting curve for each amplified PCR product and the visualization of the PCR amplicons on 2% agarose gels allowed controlling the specificity of the amplification. Relative quantification was calculated using the comparative threshold cycle ($\Delta\Delta^{CT}$) method. cDNA levels were normalized to *Gapdh* or to *Rpl19* (reference genes) and a control sample (calibrator set to 1) was used to calculate the relative values. For each gene, the PCR amplification efficiency was established from the slope of the calibration curve according to the equation: $E = 10^{(-1/slope)}$ (Pfaffl, 2004). Each reaction was done in triplicate and three–four mice per condition were analyzed.

Western blot analysis

Three mice per group were killed by cervical dislocation and retinae were quickly dissected and snap frozen in liquid nitrogen. Tissues were then homogenized in lysis buffer (20 mM Tris–HCl, 0.5% CHAPS, pH 8) containing protease inhibitors (Complete mini, Roche diagnostics) for 60 min on ice. After centrifugation for 15 min at 15,000 ×g, 4 °C, the supernatant was collected in clean eppendorf tubes, and stored at −80 °C. Protein samples (20 μg/lane) were resolved by electrophoresis on a 4–12% polyacrylamide gel and transferred to nitrocellulose

membranes. The membranes were pre-incubated in a blocking solution of 2% Top Block (Lubio Science, Lucerne, Switzerland) in TBST (Tris-base 0.1 M, 0.2% Tween-20, pH 7.4) for 1 h at room temperature, incubated with primary antibodies overnight at 4 °C and after washing, with a horseradish peroxidase-conjugated anti-mouse or anti-rabbit antibody (1:10,000–1:25,000; Pierce Biotechnology). Primary antibodies were rabbit anti-Phospho-Stat3 (1:500, Cell Signaling, #9131), rabbit anti-Stat3 (1:500, Cell Signaling, #9132), rabbit anti-CNTF (1:3,000, abcam, #ab46172), and mouse anti-glyceraldehyde-3-phosphate dehydrogenase (GAPDH, 1:10,000; abcam, #ab8245). Protein bands were detected by adding SuperSignal West Pico Chemiluminescent Substrate (Pierce) and after exposure of the blot in a Stella detector.

Results

ShH10.DH-CNTF selectively infects Müller glia and activates the Jak3/Stat3 pathway in retinal ganglion cells

Four weeks after ShH10.GFP delivery, most of the GFP expressing cell bodies were localized in the middle of the inner nuclear layer and could be stained for glutamine synthase, a marker for the Müller cells (Fig. 1A) (Dalkara et al., 2011; Klimczak et al., 2009). At this time point, ~84% of Müller cells expressed the GFP protein. Eight weeks following optic nerve crush (12 weeks post ShH10.GFP injection), a very high density of GFP-positive Müller cells was visualized by confocal microscopy on retinal flat-mounts (Fig. 1B), indicating that ShH10 can mediate long-term transgene expression in the axotomized retinae.

The modified human gene of *Cntf*, *DH-Cntf* (Saggio et al., 1995), acting as a CNTFRα super-agonist was packaged into ShH10 (Fig. 1C). CNTF signaling involves the intracellular phosphorylation of Stat3 that elicits growth gene expression in the nucleus (Fig. 1D). On the other hand, a negative feedback loop controls the duration of the Jak3/Stat3 cascade activation through the up-regulation of SOCS3 that binds to Jak3 and blocks further Stat3 phosphorylation. In particular after *DH-Cntf* gene transfer, SOCS3 up-regulation may counteract the cytokine signaling activation and thereby prevent long-term effects of DH-CNTF on neuron survival and axonal regrowth (Smith et al., 2009). Therefore, to determine if ShH10.DH-CNTF could sustain P-Stat3 activation in the retina, the level of P-Stat3 was followed by Western Blotting and immunohistochemistry four weeks after virus administration in intact and injured retinae (5 days post-lesion) (Figs. 1E,F). By Western Blotting, ShH10.DH-CNTF increased the level of the CNTF protein by more than 10 fold compared with untreated or ShH10.GFP-injected retinae (Fig. 1E). In agreement with this observation, the level of phospho-

Fig. 1. ShH10.DH-CNTF selectively infects Müller glia and activates the Jak3/Stat3 pathway in RGCs. The expression of the GFP protein was visualized by confocal microscopy on retinal cross-sections co-labeled for glutamine synthetase (GS, arrowheads) 4 weeks after intravitreous injection of ShH10.GFP (A) or on retinal flat-mounts (B) 12 weeks after intravitreous injection of ShH10.GFP and 8 weeks following optic nerve crush (ONC). C) A modified version of the human CNTF cDNA containing the signal peptide of growth hormone and 2 amino acid mutations (DH-CNTF) was packaged into ShH10 vectors. D) Scheme representing the activation of the Jak3/Stat3 pathway and its inhibitor SOCS3. E) By Western Blotting, CNTF and P-Stat3 were strongly up-regulated by ShH10.DH-CNTF. For quantitative analysis, the intensity of CNTF/GAPDH and P-Stat3/Stat3 signals was measured by densitometry in 5 and 3 separate blots respectively (mean ± S.E.M.). F) The co-localization of P-Stat3 and β3Tubulin on retinal crossections revealed the selective activation of P-Stat3 in RGCs. G) By semi-qRT-PCR, *Stat3*, *Jak3* and *Socs3* mRNAs were up-regulated by ShH10.DH-CNTF and to a lesser extent by ShH10.GFP with or without injury. Statistics: ANOVA, *: $p<0.05$; **: $p<0.01$; ***: $p<0.001$. ONL, outer nuclear layer; INL, inner nuclear layer; IPL, inner plexiform layer; GCL, ganglion cell layer; NS, not significant. Scale bars: A, B (right panel), F = 50 μm; B = 100 μm.

Stat3 was markedly up-regulated by ShH10.DH-CNTF in lesioned and intact retinae (Fig. 1E). We then localized the activation of P-Stat3 by immunofluorescence on retinal crossections (Fig. 1F). No signal could be detected in untreated or ShH10.GFP-treated retinae five days post-lesion (Fig. 1F). In contrast, in ShH10.DH-CNTF-infected retinae a strong P-Stat3 staining was exclusively present in RGCs as indicated by co-staining for β3tubulin in the intact and injured retinae at five days post-lesion. Importantly, P-Stat3 was not detectable in the inner nuclear layer where the Müller cell bodies are located.

As our Western Blot analysis revealed an elevation of Stat3 protein expression after ShH10 virus injection and injury, we wondered whether the expression of important cytokine signaling intermediates was also affected. To this aim, the levels of *Stat3*, *Jak3* and *Socs3* mRNAs (Smith et al., 2009) were assessed by qRT-PCR (Figs. 1D,G). To distinguish the impact of the GFP gene expression in Müller cells from the effect of Müller cell infection by ShH10, retinae were treated with empty ShH10 vector capsids. DH-CNTF significantly enhanced the mRNA levels of *Stat3*, *Jak3* and *Socs3* in intact and lesioned retinae compared with other treatment conditions (Fig. 1G). Interestingly, *Socs3* and *Jak3* mRNAs were increased in similar proportions, suggesting that the blockade of Jak3 by the binding of SOCS3 may be compensated by the up-regulation of Jak3 expression. ShH10.GFP also stimulated gene expression of the three molecules relative to ShH10.Empty but to a lower extent than ShH10.DH-CNTF (Fig. 1G). This suggests a possible influence of GFP expression on the RGC response to injury. Overall, these data show that Müller cell infection by ShH10.DH-CNTF enhances

the intracellular activation of the Jak3/Stat3 pathway in intact and injured retinal ganglion cells.

The Müller cell gliosis is not exacerbated by ShH10.DH-CNTF

Several studies previously reported that CNTF was a potent gliosis activator in the retina (Kirsch et al., 2010; Peterson et al., 2000; Xue et al., 2011). For example, injecting CNTF elevated the expression of the intermediate filament proteins glial fibrillary acidic protein (GFAP) and vimentin (Peterson et al., 2000; Wang et al., 2002). We thus measured the mRNA levels of *Gfap* and *vimentin* in intact and optic nerve crushed retinal lysates (Figs. 2A–B). In the intact retinae, the levels of *Gfap* and *vimentin* mRNA were higher in retinae treated with either ShH10.GFP or ShH10.DH-CNTF than in those left untreated or receiving the empty ShH10 vector. Surprisingly, however, the administration of ShH10.GFP up-regulated more *Gfap* and *vimentin* mRNAs than ShH10.DH-CNTF with or without optic nerve crush (Figs. 2A,B). On retinal crossections, GFAP immunofluorescence was prominent in the astrocytes of the optic fiber layer in all injured retinae (Fig. 2C, arrow), but it only appeared in the reactive Müller glia of animals treated with ShH10.GFP (Fig. 2C, arrowheads). In agreement with the qRT-PCR data, immunofluorescent labeling showed weaker GFAP activation for the ShH10.DH-CNTF-treated retinae than in those receiving ShH10.GFP. Together, these data suggest that Müller cell-mediated DH-CNTF delivery does not enhance gliosis contrary to the GFP gene transfer with ShH10.
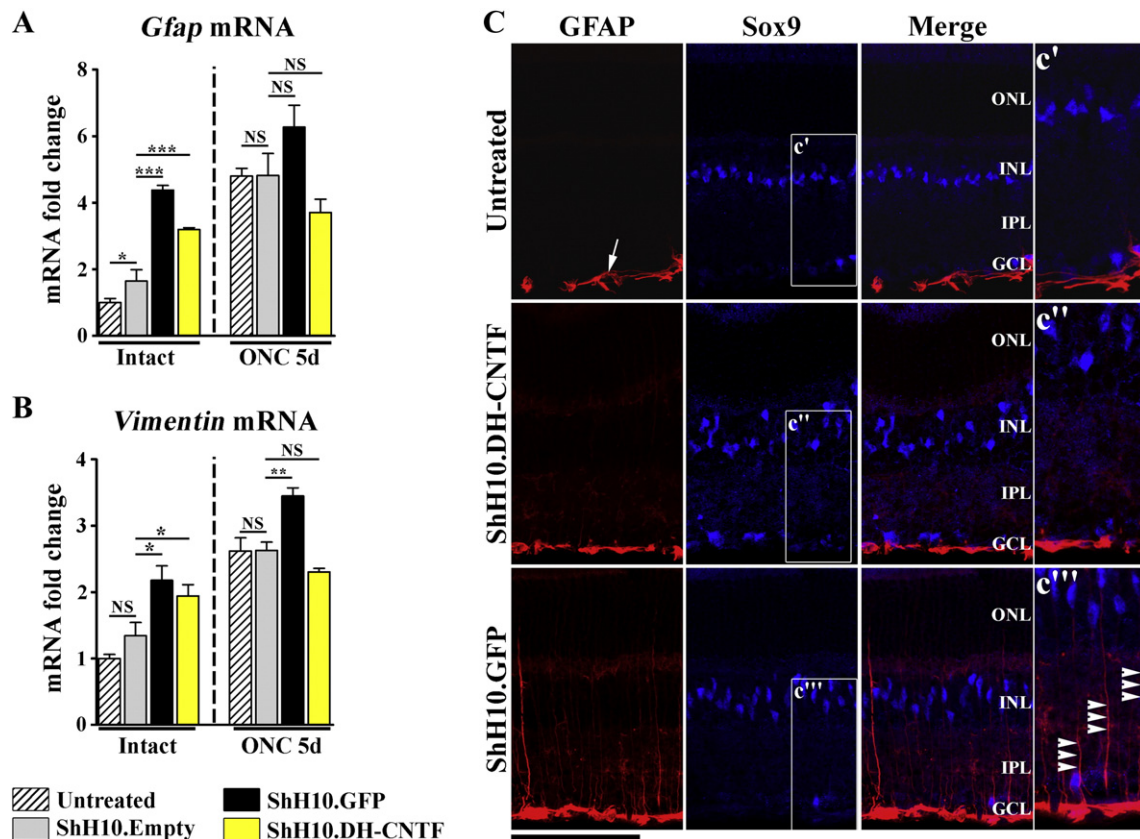

Fig. 2. Analysis of gliosis in ShH10-treated retinae. A–B) The mRNA levels of *Gfap* and *vimentin* were determined by semi-qRT-PCR in intact retinae and 5 days after optic nerve crush. Before lesion, ShH10.GFP and ShH10.DH-CNTF caused a significant elevation of *Gfap* and *vimentin* expression compared with empty ShH10 virus. After crush lesion, ShH10.GFP but not ShH10.DH-CNTF induced more *Gfap* and *vimentin* transcript up-regulations than in ShH10.Empty-treated retinae (ANOVA, *: $p<0.05$; **: $p<0.01$; ***: $p<0.001$). C) Immunofluorescent stainings on retinal crossections showed a stronger signal for GFAP in the radial processes of the Müller glia (arrowheads) with ShH10.GFP, 5 days after injury than in other conditions. The nuclei of the glial cells were labeled with Sox9, a transcription factor specifically expressed in the Müller glia in the inner nuclear layer. Magnified views are shown on the right-hand side in c′, c″ and c‴. ONL, outer nuclear layer; INL, inner nuclear layer; IPL, inner plexiform layer; GCL, ganglion cell layer; NS, not significant. Scale bar: C = 100 μm.

ShH10.DH-CNTF enhances survival of retinal ganglion cells after optic nerve lesion

Retinal ganglion cells die rapidly and massively after optic nerve lesion. Possible survival effects on RGCs were examined by staining retinal flat-mounts for β3tubulin at 2 and 8 weeks after optic nerve injury (Fig. 3). At the two time points, the density of RGCs was much higher in retinae treated with ShH10.DH-CNTF than in those infected with ShH10.GFP or the untreated ones (Figs. 3A–D). The neuroprotective effect of ShH10.DH-CNTF was particularly strong at 2 weeks, a time where $2{,}003 \pm 25$ RGCs/mm^2 (S.E.M., n = 5) remained alive compared to 658 ± 66 RGCs/mm^2 (S.E.M., n = 5) in the untreated and 816 ± 63 RGCs/mm^2 (S.E.M., n = 4) in the ShH10.GFP-treated mice (Figs. 3A,B,E). The number of surviving RGCs was lower at 8 weeks, but ShH10.DH-CNTF still increased the number of surviving neurons (722 ± 15, S.E.M., n = 6) by 1.5 fold and 2 fold, respectively, compared to ShH10.GFP (479 ± 46, S.E.M., n = 3) or the untreated group (348 ± 32, S.E.M., n = 4) (Figs. 3C,D,E). In addition, eight weeks after axonal injury, some RGC cell bodies showed abnormally big cell bodies surrounded by a high density of sprouted fibers (Fig. 3D). The measurement of the cell body diameters revealed that ShH10.DH-CNTF treated retinae had a higher proportion of large diameter RGCs (Figs. 3C,D,F). This may be due to a size increase by CNTF or to the preferential survival of large RGCs. This soma size increase was important enough to significantly affect the average soma diameter (Fig. 3F). Of note, ShH10.GFP slightly increased neuronal survival and the soma diameters at 8 weeks post-lesion, suggesting once again that the ectopic expression of GFP in retinal glia can exert some unexpected but positive effects on the preservation of injured RGCs. These observations reveal potent and long-lasting survival effects induced by the glial cell infection with ShH10.DH-CNTF.

ShH10.DH-CNTF is sufficient to promote long-distance axonal regeneration in the optic nerve after crush injury

To determine if DH-CNTF could activate axonal regeneration 2 and 8 weeks after optic nerve crush, cholera toxin beta subunit coupled to alexa-594 (CTb) was intravitreously delivered one day (2-weeks groups) or 2 days (8-weeks groups) before perfusion. Very few axonal processes were detectable beyond the injury site of control animals receiving ShH10.GFP (Fig. 4A) or of untreated injured mice (Fig. 4B). In contrast, mice injected with ShH10.DH-CNTF showed many CTb-labeled fibers crossing the lesion site and extending into the distal optic nerve 2 weeks after crush (Fig. 4C). Eight weeks after injury, many axons were observed 3 mm past the lesion site (Fig. 4E, e′) and some of them reached the optic chiasm (Fig. 4E, e″) at a distance of
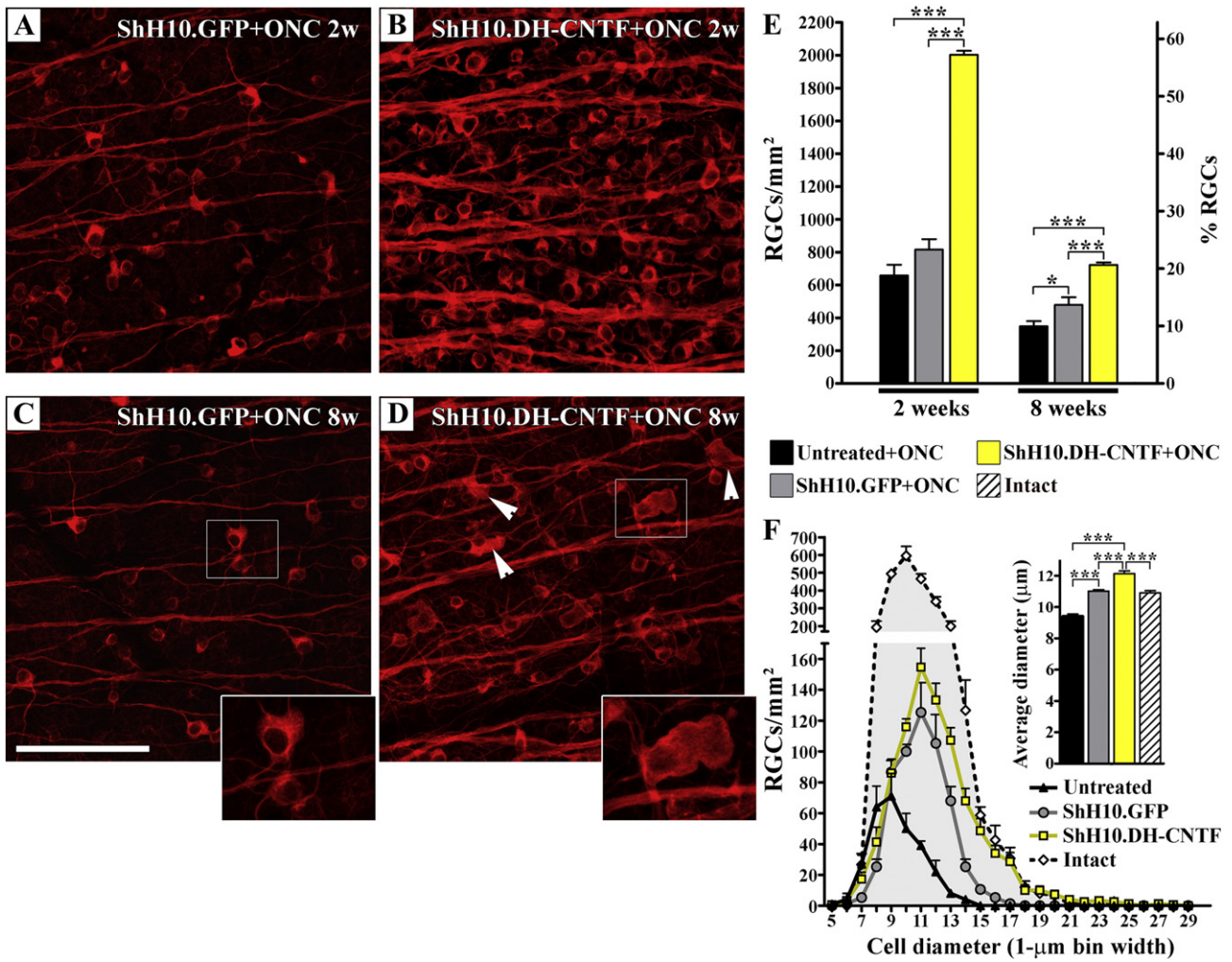

Fig. 3. ShH10-mediated delivery of DH-CNTF promotes robust and sustained survival of axotomized retinal ganglion cells. A–D) The survival of retinal ganglion cells was observed 2 and 8 weeks after optic nerve crush on retinal flat-mounts by immunofluorescent staining for β3Tubulin. D) The somata of ShH10.DH-CNTF-stimulated cells appeared bigger (arrowheads) than in other injured groups. E) Quantitatively, after the administration of ShH10.DH-CNTF the density of surviving RGCs was significantly higher at 2 weeks and 8 weeks post-lesion than in untreated or ShH10.GFP-treated retinae (ANOVA, *: p<0.05; ***: p<0.001). F) The cell diameter distribution was assessed for the different experimental groups. The average diameter of RGCs was statistically larger after ShH10.DH-CNTF than after ShH10.GFP injection (ANOVA, ***: p<0.001). Scale bars: A–D = 100 μm.
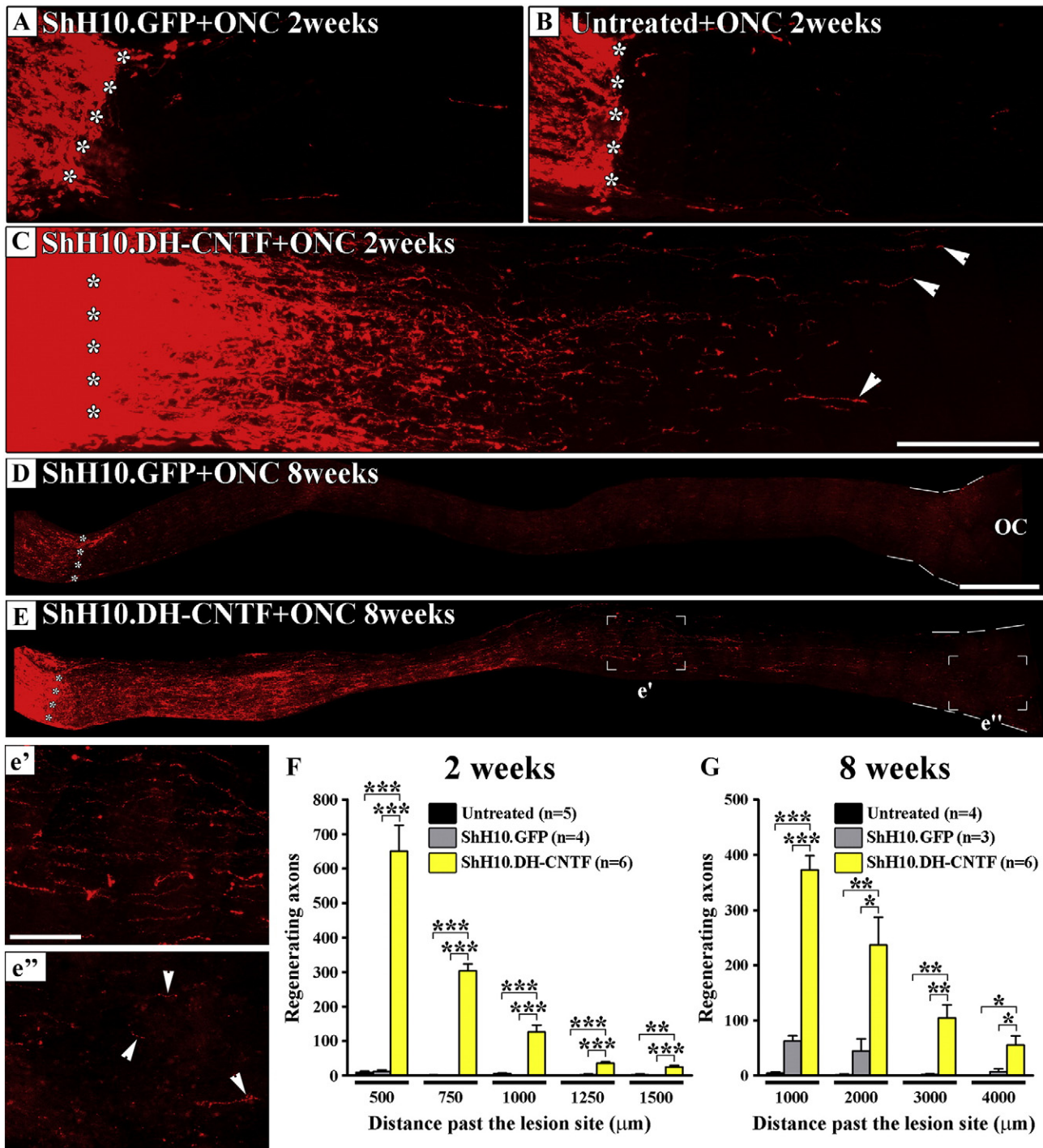
Fig. 4. Retinal ganglion cell axon growth is strongly stimulated by ShH10.DH-CNTF. Axonal growth was followed in the optic nerve by anterograde tracing with cholera toxin b subunit (A–E). The lesion site is indicated by white stars. A–E) In the optic nerve, the effects of ShH10.DH-CNTF on axonal regeneration were examined 2 and 8 weeks post-lesion relative to the control virus ShH10.GFP or to the absence of treatment. e′, e″) Close-up from E) showing axonal fibers present at ~3 mm and ~4.5 mm, close to the optic chiasm (OC), respectively. F) Quantitatively, ShH10.DH-CNTF induced significantly more axonal growth than control treatments up to a distance of 1.5 mm past the lesion site, 2 weeks post-crush (ANOVA, **: $p < 0.01$; ***:$p < 0.001$). G) Eight weeks after injury, regenerated fibers were significantly more numerous with ShH10.DH-CNTF at 4 mm past the lesion site than with other treatments (ANOVA, *:$p < 0.05$; **: $p < 0.01$; ***:$p < 0.001$). Scale bars: A–C = 200 μm; D–E = 400 μm; e′, e″ = 100 μm.

Fig. 5. ShH10.DH-CNTF preserves the regenerated axons in the whole-mounted optic nerve after 6 months. A) RGCs were infected by an intraocular injection of AAV2.GFP five months after injury and the unsectioned optic nerve was analyzed by confocal microscopy at 6 months. B–I) Complete optic nerve reconstruction allowed us to observe GFP-containing axons at different levels in the optic nerves. The lesion site was indicated with a white star. C) At >5 mm past the lesion site, axons extended ipsilaterally or contralaterally (arrows) while some fibers exhibited U-turn shapes (arrowhead). D–I) The superimposition of autofluorescent structures in red (excitation at 532 nm) and of GFP in green revealed the high density of regenerated axons in optic nerve. J–L) At different distances from the lesion, like here at ~2 mm, axons underlined in colors showed regular and straight shapes (arrows) while some formed loops (arrowheads). Scale bars: B = 0.5 mm; C = 100 μm, D–L = 50 μm.
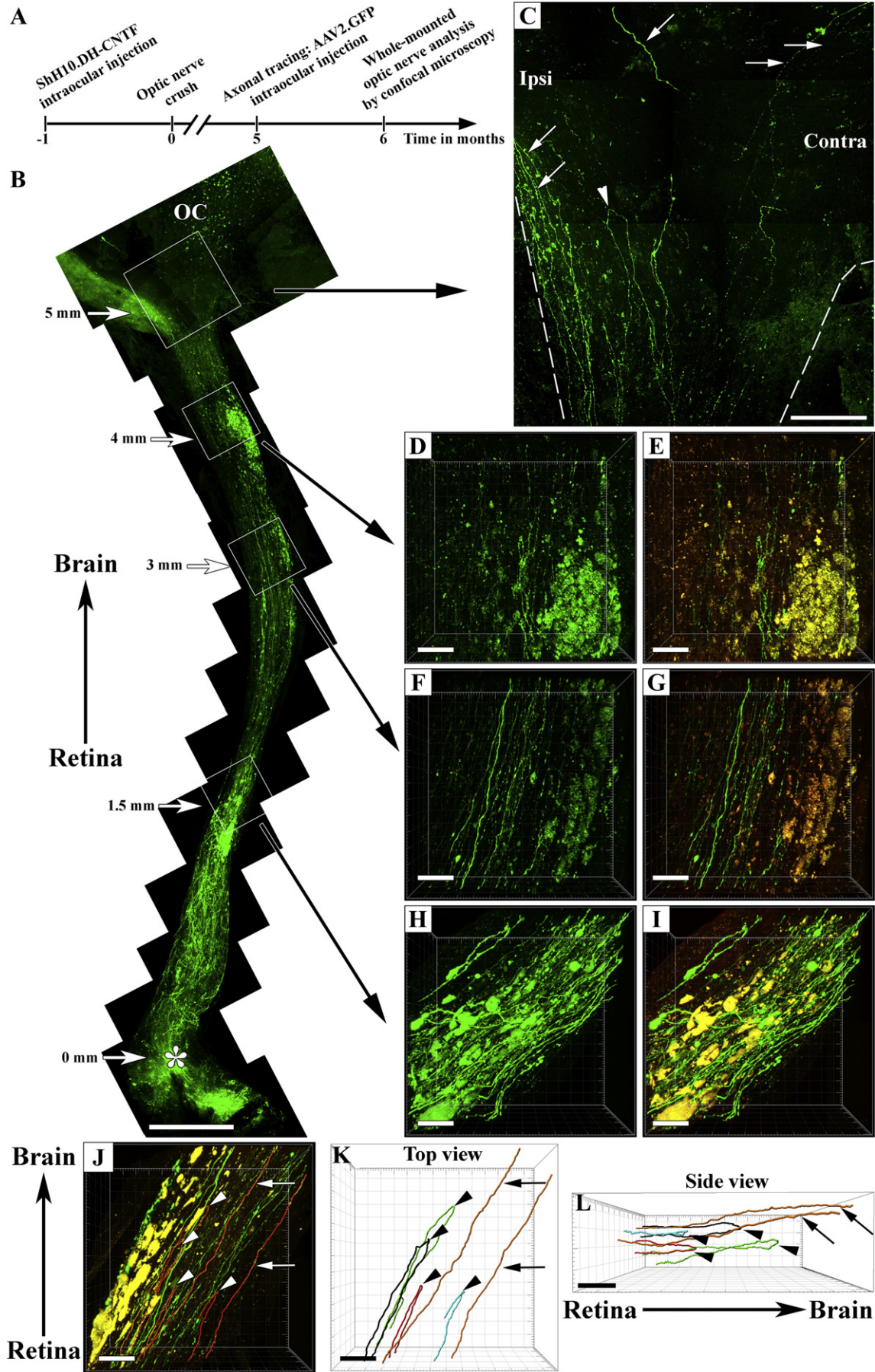
~4.5 mm. In several mice, regenerating axons, characterized by their typical irregular trajectory and their thin diameter, were present within the optic chiasm. In contrast to the DH-CNTF animals, ShH10.GFP treated mice showed only very few axons (Fig. 4D). Quantitatively, ShH10.DH-CNTF enabled CTb-labeled axons to regenerate up to 1.5 mm by 2 weeks after injury, while after 8 weeks axons extended to 4 mm and beyond (Figs. 4F,G).

Long-term effect of ShH10.DH-CNTF and aberrant trajectories of regenerating axons in the optic tract

Ultimately, gene therapy in the damaged CNS is aimed at promoting life-long lasting neuronal repair. So far, the benefits of growth-inducing molecules have never been studied over a long period of time. This is particularly relevant as the very slow Wallerian degeneration in injured CNS white matter may impact the maintenance of regenerated axons (Ludwin, 1990). We determined if regenerated axons were still present in the optic nerve 6 months after injury. RGC axons were labeled by intravitreally injecting AAV2.GFP virus at five months post-lesion and the optic nerve was analyzed one month later (Fig. 5A). In order to follow the course of single axons, whole, unsectioned optic nerves were examined by confocal microscopy and analyzed in 3D with the Imaris software. The 5 optic nerves observed at 6 months presented strong atrophy as a result of Wallerian degeneration that made the optic nerve transparent. The full reconstruction of the optic nerves revealed the presence of many axons that had regenerated beyond the lesion site (Figs. 5B,D–I). Some of them extended through the optic chiasm and continued into the contralateral or ipsilateral optic tracts (see arrows, Fig. 5C). The persistence of re-grown axons all along the optic nerve suggests that ShH10.DH-CNTF not only activates axon growth and regeneration but also promotes their survival over a very long period of the animal's life. Importantly, many of the axons had straight, unbranched morphologies while others consistently formed conspicuous loops or "U-turns" at varying distances from the lesion and the chiasm (Figs. 5C,J–L). Three dimensional quantitative analysis of axons at 3 mm from the injury site revealed that 16 axons formed U-turns while 30 axons grew straight through the optic nerve segment examined in 4 mice. This suggests that ~35% of growing axons extended in the wrong direction at relatively long distances. Autofluorescent structures, probably macrophages and myelin remnants, were detected with an excitation wavelength of 532 nm throughout the optic nerve (Figs. 5E,G,I,J).

Aberrant axonal sprouting at the retinal surface 8 weeks after injury

Interestingly, the robust growth-promoting effect of DH-CNTF was not restricted to the optic nerve; massive intraocular sprouting of β3Tubulin-positive RGC fibers was systematically observed in mice injected with ShH10.DH-CNTF (Fig. 6B) while virtually no intraocular axon outgrowth was visible following ShH10.GFP administration (Fig. 6A). In addition, intact retinae did not exhibit outgrowth after ShH10.DH-CNTF delivery, suggesting that axonal outgrowth in the retina depends on axonal injury. The neurite sprouting covered the normal axon fascicles of the optic fiber layer, and abundant sprouting fibers appeared intermingled around the optic nerve head (Fig. 6B). Elongated fibers were also seen in bundles at the surface of the veins in the periphery of the retina (Fig. 6B, magnified pictures). Six months after injury, many ectopic β3tubulin-labeled sprouts and axons induced by ShH10.DH-CNTF were still present within the eye at the inner surface of the retina and on the blood vessels (Figs. 6C–F). These data demonstrate that ShH10.DH-CNTF can induce powerful regeneration of severed axons in the optic nerve, but it also causes abundant aberrant sprouting of axons within the eye.

Discussion

By selectively and efficiently infecting the retinal glial cells with a new AAV variant, we could deliver the CNTFRα super-agonist DH-CNTF to RGCs thereby causing a long-lasting and potent activation of the Jak3/Stat3 pathway, a key regulator of neuronal growth. ShH10.DH-CNTF induced long-distance, sustained axonal regeneration through the crushed optic nerve and into the optic chiasm. It also had neuroprotective effects on axotomized RGCs. Interestingly, the strong stimulation of neurite growth by ShH10.DH-CNTF also led to massive ectopic sprouting in the retina, a phenomenon that was never reported so far. Within the optic nerve the regenerating fibers frequently formed U-turns and grew back towards the lesion site. These results show that axonal misguidance is a new and important parameter limiting the effects of growth stimulatory factors on long-range axonal regeneration in the CNS.

The extent of neuronal survival after injury, and the magnitude of retinal ganglion cell axonal regeneration observed in the present study are higher than what has been obtained so far with intravitreal injections of recombinant CNTF peptides or other neurotrophic factors (Lingor et al., 2008; Mansour-Robaey et al., 1994; Sapieha et al., 2003). Two factors may be crucial for this result: DH-CNTF binds the receptor component CNTFRα with higher affinity than native mouse CNTF, i.e. acts as a super-agonist, and the AAV variant ShH10 is highly selective for retinal Müller cells which it infects with very high efficiency. Müller cell processes wrap the RGC cell bodies closely; in this way, high concentrations of CNTF are delivered locally and continuously to the RGCs. Accordingly, ShH10.DH-CNTF strongly up-regulated the expression of *Stat3*, *Jak3* and *Socs3* in the RGCs, typical components of the CNTF/cytokine signaling pathway. The high level of P-Stat3 indicates that feedback-inhibition via SOCS3 did not block the cytokine pathway possibly because of the strong up-regulations of *Stat3* and *Jak3*. Thus, the ShH10 vector appears as an excellent tool for gene therapy in the retina, in particular for Müller cells and RGCs. The availability of glia-infecting ShH10 in conjunction with RGC-targeting AAV2 vectors offers the new possibility of improving RGC axon regeneration and survival by combining intracellular and extracellular stimulations.

It is not clear why Müller cell gliosis was enhanced after injury with ShH10.GFP. The absence of gliosis exacerbation with ShH10.DH-CNTF may be due to the fact that CNTF is a secreted protein, contrary to GFP that accumulates in the cytoplasm. It could be that up-regulated intermediate filament proteins during gliosis such as GFAP or vimentin interact with GFP in the Müller cell cytoplasm and thereby cause cell stress and potentiate glial cell reaction. It has previously been reported that transfecting neuronal and non-neuronal cells with GFP could cause adverse effects. For example, the co-expression of GFP and beta-galactosidase in mouse brains led to the formation of ubiquitin-positive aggregates that were associated with gliosis activation (Krestel et al., 2004). In myoblasts, GFP was shown to impair actin–myosin interaction and therefore muscle cell contractility (Agbulut et al., 2006).

ShH10.DH-CNTF had a robust neuroprotective effect for RGCs after complete optic nerve lesion. In the clinically more relevant conditions of milder trauma or glaucoma, ShH10.DH-CNTF may prevent or delay RGC death at a very important degree. ShH10.DH-CNTF also seemed to have a general trophic effect on the RGC cell bodies as suggested by the presence of very large cells and the size shift in the surviving population, although for the latter effect a selective survival action of DH-CNTF on the population of large RGCs cannot be excluded.

DH-CNTF supplied by the Müller cells induced a massive regenerative response of the transected RGC axons; many axons reached the optic chiasm 8 weeks after lesion (≥4 mm of regeneration). The observed regeneration was comparable in intensity to the deletion of *Pten* gene reported by Kurimoto et al. (2010) but much less than that reported by Park et al. (2008). The activation of Stat3 in RGCs by the ablation of the *Socs3* gene (Smith et al., 2009) led to a very similar axon regeneration as the one obtained in the present study with ShH10.DH-CNTF suggesting that DH-CNTF can directly mediate its growth effect via

Fig. 6. Intraocular axonal growth stimulation by ShH10.DH-CNTF. A, B) At 8 weeks after injury, in the retina treated with ShH10.DH-CNTF β3Tubulin-stained axons massively sprouted around the optic disk (OD) and spread preferentially along the veins delineated by a white dotted line. To visualize axonal outgrowth at the surface of the retina, confocal image stacks were acquired above the RGC and fiber layers. Close-ups from B showing magnified axonal stream on veins (arrows) and bulbous terminals (arrowhead). At 6 months after optic nerve crush, the retinal blood vessels were labeled by intracardially perfusing animals with lectin-FITC (C) before PFA fixation and the retinal ganglion cell axons were stained for β3Tubulin (D). The two stainings were imaged on retinal flat-mounts with a confocal microscope. E) The superimposition of the lectin-FITC (*Lycopersicon esculentum*) and β3Tubulin signals showed many axons at the surface of the veins. F) Close-up from E (dotted area) showing magnified β3Tubulin-positive axonal stream on a vein labeled by lectin-FITC. Scale bars: A, B = 200 μm; C–F = 100 μm.

the intracellular activation of the Jak/Stat3 pathway in neurons. RGC infection with AAV2.CNTF was previously shown to stimulate axonal regeneration in a range of several millimeters in mice (Leaver et al., 2006a) and rats (Leaver et al., 2006b). However, we cannot directly compare the magnitude of axonal regeneration observed in our study with that reported by Leaver et al. (2006a) because 1) we used different methods of axonal labeling, 2) Leaver and co-workers did not provide quantitative data for long distances, e. g. at 3 mm and 4 mm after the injury site and 3) we examined axonal growth up to 8 weeks after lesion while the other group looked after 5 weeks. Nevertheless, clear differences exist between the effects of AAV2.CNTF and ShH10.DH-CNTF. For example, contrary to ShH10.DH-CNTF, AAV2.CNTF did not significantly increase Socs3 mRNA expression and was not reported to cause intraocular axonal outgrowth (Hellstrom et al., 2011). Those two events may reflect the stronger stimulation of cytokine signaling and axonal growth by ShH10.DH-CNTF. In addition, it is not known if the stimulation of CNTF secretion by AAV2.CNTF potentiates gliosis in axotomized retinae and if this viral serotype is as selective to stimulate P-Stat3 in RGCs as ShH10.DH-CNTF. At 6 months after lesion, many regenerated axons survived in the optic nerve, the chiasm and the contra- and ipsilateral optic tracts, showing a sustainable effect of the CNFT treatment.

By analyzing the course of individual axons in whole nerve mounts in three dimensions at 6 months post-lesion, we observed that many regenerated axons formed U-turns in the optic nerve. If such a phenomenon also occurs with other growth stimulatory treatments (Kurimoto et al., 2010; Leaver et al., 2006b; Park et al., 2008; Smith et al., 2009), reported axon counts are significantly flawed. More importantly, the phenomenon shows that guidance mechanisms that are crucial during development are altered or absent in the adult, injured nerve. Inhibitory cues like Nogo-A, MAG, and OMgp on myelin debris (Schwab, 2010) or ephrinB3 (Duffy et al., 2012) and sema5A (Goldberg et al., 2004) may additionally repel the growth cones of the regenerating axons, thereby causing their misguidance. Our recent, unpublished data indicate that blocking intracellular mechanisms involved in growth cone collapse and axonal growth inhibition can improve axonal regeneration by reducing axonal U-turns.

An additional unexpected finding was the massive sprouting in the retina (but not the optic nerve) possibly originating from optic nerve axonal U-turns or from collaterals of retinal axon bundles. Whether such aberrant growth also occurs with other growth stimulatory treatments (Park et al., 2008; Smith et al., 2009) has not been reported so far and needs to be investigated. If these sprouts form synaptic contacts and might interfere with retinal function remains to be analyzed. The successful long-range axonal regeneration and ultimately the reconnection of retinal axons with brain targets will depend on the control of axonal guidance and not only on the growth state induction.

In summary, our data show that a single, optimized neurotrophic factor, DH-CNTF, applied by a cell type-specific AAV-derived virus to the retinal glia that tightly wraps the retinal ganglion cells, enhances neuronal survival and induces persistent optic axon regeneration into and beyond the chiasm in adult mice. AAV constructs do not induce inflammation and are used clinically, thus, these results may have clinical potential for optic nerve lesions by trauma or local inflammation as well as for slow degenerative diseases like glaucoma. However, the present results also show that a very strong stimulation of growth can trigger ectopic sprouting of axons e.g. on the retina. In the optic nerve many axons lost directionality and were misguided, pointing to an important role of guidance mechanisms for regenerating axons, a problem that deserves to be further studied in other adult CNS regions where it has been largely disregarded up to now.

Acknowledgments

References

Agbulut, O., Coirault, C., Niederlander, N., Huet, A., Vicart, P., Hagege, A., Puceat, M., Menasche, P., 2006. GFP expression in muscle cells impairs actin-myosin interactions: implications for cell therapy. Nat. Methods 3, 331.

Bainbridge, J.W., Smith, A.J., Barker, S.S., Robbie, S., Henderson, R., Balaggan, K., Viswanathan, A., Holder, G.E., Stockman, A., Tyler, N., Petersen-Jones, S., Bhattacharya, S.S., Thrasher, A.J., Fitzke, F.W., Carter, B.J., Rubin, G.S., Moore, A.T., Ali, R.R., 2008. Effect of gene therapy on visual function in Leber's congenital amaurosis. N. Engl. J. Med. 358, 2231–2239.

Benowitz, L.I., Yin, Y., 2007. Combinatorial treatments for promoting axon regeneration in the CNS: strategies for overcoming inhibitory signals and activating neurons' intrinsic growth state. Dev. Neurobiol. 67, 1148–1165.

Berkelaar, M., Clarke, D.B., Wang, Y.C., Bray, G.M., Aguayo, A.J., 1994. Axotomy results in delayed death and apoptosis of retinal ganglion cells in adult rats. J. Neurosci. 14, 4368–4374.

Bringmann, A., Pannicke, T., Grosche, J., Francke, M., Wiedemann, P., Skatchkov, S.N., Osborne, N.N., Reichenbach, A., 2006. Muller cells in the healthy and diseased retina. Prog. Retin. Eye Res. 25, 397–424.

Cheng, L., Sapieha, P., Kittlerova, P., Hauswirth, W.W., Di Polo, A., 2002. TrkB gene transfer protects retinal ganglion cells from axotomy-induced death in vivo. J. Neurosci. 22, 3977–3986.

Cui, Q., Yip, H.K., Zhao, R.C., So, K.F., Harvey, A.R., 2003. Intraocular elevation of cyclic AMP potentiates ciliary neurotrophic factor-induced regeneration of adult rat retinal ganglion cell axons. Mol. Cell. Neurosci. 22, 49–61.

Dalkara, D., Kolstad, K.D., Caporale, N., Visel, M., Klimczak, R.R., Schaffer, D.V., Flannery, J.G., 2009. Inner limiting membrane barriers to AAV-mediated retinal transduction from the vitreous. Mol. Ther. 17, 2096–2102.

Dalkara, D., Kolstad, K.D., Guerin, K.I., Hoffmann, N.V., Visel, M., Klimczak, R.R., Schaffer, D.V., Flannery, J.G., 2011. AAV mediated GDNF secretion from retinal glia slows down retinal degeneration in a rat model of retinitis pigmentosa. Mol. Ther. 19, 1602–1608.

Dittrich, F., Thoenen, H., Sendtner, M., 1994. Ciliary neurotrophic factor: pharmacokinetics and acute-phase response in rat. Ann. Neurol. 35, 151–163.

Duffy, P., Wang, X., Siegel, C.S., Tu, N., Henkemeyer, M., Cafferty, W.B., Strittmatter, S.M., 2012. Myelin-derived ephrinB3 restricts axonal regeneration and recovery after adult CNS injury. Proc. Natl. Acad. Sci. U. S. A. 109, 5063–5068.

Goldberg, J.L., Vargas, M.E., Wang, J.T., Mandemakers, W., Oster, S.F., Sretavan, D.W., Barres, B.A., 2004. An oligodendrocyte lineage-specific semaphorin, Sema5A, inhibits axon growth by retinal ganglion cells. J. Neurosci. 24, 4989–4999.

Grieger, J.C., Choi, V.W., Samulski, R.J., 2006. Production and characterization of adeno-associated viral vectors. Nat. Protoc. 1, 1412–1428.

Harvey, A.R., Hu, Y., Leaver, S.G., Mellough, C.B., Park, K., Verhaagen, J., Plant, G.W., Cui, Q., 2006. Gene therapy and transplantation in CNS repair: the visual system. Prog. Retin. Eye Res. 25, 449–489.

Hellstrom, M., Muhling, J., Ehlert, E.M., Verhaagen, J., Pollett, M.A., Hu, Y., Harvey, A.R., 2011. Negative impact of rAAV2 mediated expression of SOCS3 on the regeneration of adult retinal ganglion cell axons. Mol. Cell. Neurosci. 46, 507–515.

Jahrling, N., Becker, K., Dodt, H.U., 2009. 3D-reconstruction of blood vessels by ultramicroscopy. Organogenesis 5, 145–148.

Kirsch, M., Trautmann, N., Ernst, M., Hofmann, H.D., 2010. Involvement of gp130-associated cytokine signaling in Muller cell activation following optic nerve lesion. Glia 58, 768–779.

Klimczak, R.R., Koerber, J.T., Dalkara, D., Flannery, J.G., Schaffer, D.V., 2009. A novel adeno-associated viral variant for efficient and selective intravitreal transduction of rat Muller cells. PLoS One 4, e7467.

Krestel, H.E., Mihaljevic, A.L., Hoffman, D.A., Schneider, A., 2004. Neuronal co-expression of EGFP and beta-galactosidase in mice causes neuropathology and premature death. Neurobiol. Dis. 17, 310–318.

Kurimoto, T., Yin, Y., Omura, K., Gilbert, H.Y., Kim, D., Cen, L.P., Moko, L., Kugler, S., Benowitz, L.I., 2010. Long-distance axon regeneration in the mature optic nerve: contributions of oncomodulin, cAMP, and pten gene deletion. J. Neurosci. 30, 15654–15663.

Leaver, S.G., Cui, Q., Bernard, O., Harvey, A.R., 2006a. Cooperative effects of bcl-2 and AAV-mediated expression of CNTF on retinal ganglion cell survival and axonal regeneration in adult transgenic mice. Eur. J. Neurosci. 24, 3323–3332.

Leaver, S.G., Cui, Q., Plant, G.W., Arulpragasam, A., Hisheh, S., Verhaagen, J., Harvey, A.R., 2006b. AAV-mediated expression of CNTF promotes long-term survival and regeneration of adult rat retinal ganglion cells. Gene Ther. 13, 1328–1341.

Leon, S., Yin, Y., Nguyen, J., Irwin, N., Benowitz, L.I., 2000. Lens injury stimulates axon regeneration in the mature rat optic nerve. J. Neurosci. 20, 4615–4626.

Lingor, P., Tonges, L., Pieper, N., Bermel, C., Barski, E., Planchamp, V., Bahr, M., 2008. ROCK inhibition and CNTF interact on intrinsic signalling pathways and differentially regulate survival and regeneration in retinal ganglion cells. Brain 131, 250–263.

Ludwin, S.K., 1990. Oligodendrocyte survival in Wallerian degeneration. Acta Neuropathol. (Berl) 80, 184–191.

Maguire, A.M., Simonelli, F., Pierce, E.A., Pugh Jr., E.N., Mingozzi, F., Bennicelli, J., Banfi, S., Marshall, K.A., Testa, F., Surace, E.M., Rossi, S., Lyubarsky, A., Arruda, V.R., Konkle, B., Stone, E., Sun, J., Jacobs, J., Dell'Osso, L., Hertle, R., Ma, J.X., Redmond, T.M., Zhu, X., Hauck, B., Zelenaia, O., Shindler, K.S., Maguire, M.G., Wright, J.F., Volpe, N.J., McDonnell, J.W., Auricchio, A., High, K.A., Bennett, J., 2008. Safety and efficacy of gene transfer for Leber's congenital amaurosis. N. Engl. J. Med. 358, 2240–2248.

Maguire, A.M., High, K.A., Auricchio, A., Wright, J.F., Pierce, E.A., Testa, F., Mingozzi, F., Bennicelli, J.L., Ying, G.S., Rossi, S., Fulton, A., Marshall, K.A., Banfi, S., Chung, D.C., Morgan, J.I., Hauck, B., Zelenaia, O., Zhu, X., Raffini, L., Coppieters, F., De Baere, E.,

Shindler, K.S., Volpe, N.J., Surace, E.M., Acerra, C., Lyubarsky, A., Redmond, T.M., Stone, E., Sun, J., McDonnell, J.W., Leroy, B.P., Simonelli, F., Bennett, J., 2009. Age-dependent effects of RPE65 gene therapy for Leber's congenital amaurosis: a phase 1 dose-escalation trial. Lancet 374, 1597–1605.

Mansour-Robaey, S., Clarke, D.B., Wang, Y.-C., Bray, G.M., Aguayo, A.J., 1994. Effects of ocular injury and administration of brain-derived neurotrophic factor on survival and regrowth of axotomized retinal ganglion cells. Proc. Natl. Acad. Sci. U.S.A. 91, 1632–1636.

Muller, A., Hauk, T.G., Fischer, D., 2007. Astrocyte-derived CNTF switches mature RGCs to a regenerative state following inflammatory stimulation. Brain 130, 3308–3320.

Muller, A., Hauk, T.G., Leibinger, M., Marienfeld, R., Fischer, D., 2009. Exogenous CNTF stimulates axon regeneration of retinal ganglion cells partially via endogenous CNTF. Mol. Cell. Neurosci. 41, 233–246.

Park, K.K., Liu, K., Hu, Y., Smith, P.D., Wang, C., Cai, B., Xu, B., Connolly, L., Kramvis, I., Sahin, M., He, Z., 2008. Promoting axon regeneration in the adult CNS by modulation of the PTEN/mTOR pathway. Science 322, 963–966.

Pernet, V., Hauswirth, W.W., Di Polo, A., 2005. Extracellular signal-regulated kinase 1/2 mediates survival, but not axon regeneration, of adult injured central nervous system neurons in vivo. J. Neurochem. 93, 72–83.

Peterson, W.M., Wang, Q., Tzekova, R., Wiegand, S.J., 2000. Ciliary neurotrophic factor and stress stimuli activate the Jak-STAT pathway in retinal neurons and glia. J. Neurosci. 20, 4081–4090.

Pfaffl, M.W., 2004. Quantification strategies in real-time PCR. In: Bustin, S. (Ed.), A–Z of Quantitative PCR. International University Line (IUL), La Jolla, CA, USA, pp. 87–112.

Saggio, I., Gloaguen, I., Poiana, G., Laufer, R., 1995. CNTF variants with increased biological potency and receptor selectivity define a functional site of receptor interaction. EMBO J. 14, 3045–3054.

Sapieha, P.S., Peltier, M., Rendahl, K.G., Manning, W.C., Di Polo, A., 2003. Fibroblast growth factor-2 gene delivery stimulates axon growth by adult retinal ganglion cells after acute optic nerve injury. Mol. Cell. Neurosci. 24, 656–672.

Schwab, M.E., 2010. Functions of Nogo proteins and their receptors in the nervous system. Nat. Rev. Neurosci. 11, 799–811.

Smith, P.D., Sun, F., Park, K.K., Cai, B., Wang, C., Kuwako, K., Martinez-Carrasco, I., Connolly, L., He, Z., 2009. SOCS3 deletion promotes optic nerve regeneration in vivo. Neuron 64, 617–623.

Wang, Y., Smith, S.B., Ogilvie, J.M., McCool, D.J., Sarthy, V., 2002. Ciliary neurotrophic factor induces glial fibrillary acidic protein in retinal Muller cells through the JAK/STAT signal transduction pathway. Curr. Eye Res. 24, 305–312.

Wohl, S.G., Schmeer, C.W., Kretz, A., Witte, O.W., Isenmann, S., 2009. Optic nerve lesion increases cell proliferation and nestin expression in the adult mouse eye in vivo. Exp. Neurol. 219, 175–186.

Xue, W., Cojocaru, R.I., Dudley, V.J., Brooks, M., Swaroop, A., Sarthy, V.P., 2011. Ciliary neurotrophic factor induces genes associated with inflammation and gliosis in the retina: a gene profiling study of flow-sorted, Muller cells. PLoS One 6, e20326.